Journal of proteome research

Article

pubs.acs.org/jpr

Unbiased Metabolomic Investigation of Alzheimer's Disease Brain Points to Dysregulation of Mitochondrial Aspartate Metabolism

Giuseppe Paglia,[†,‡] Matteo Stocchero,[§] Stefano Cacciatore,[∥] Steven Lai,[⊥] Peggi Angel,[#] Mohammad Tauqeer Alam,[▽] Markus Keller,[▽] Markus Ralser,[▽,○] and Giuseppe Astarita*[,⊥,◆]

[†]Center for Biomedicine, European Academy of Bolzano/Bozen, Via Galvani 31, 39100 Bolzano, Italy

[‡]Center for Systems Biology, University of Iceland, Sturlugata 8, IS 101 Reykjavik, Iceland

[§]S-IN Soluzioni Informatiche S.r.l., via G. Ferrari 14, 36100 Vicenza, Italy

[∥]Institute of Reproductive and Developmental Biology, Imperial College London, London SW7 2AZ, United Kingdom

[⊥]Waters Corporation, Milford, Massachusetts 01757, United States

[#]Protea Biosciences Group, Incorporated Morgantown, West Virginia 26505, United States

[▽]Department of Biochemistry and Cambridge Systems Biology Centre, University of Cambridge, 80 Tennis Court Road, Cambridge CB2 1GA, United Kingdom

[○]Mill Hill Laboratory, The Francis Crick Institute, The Ridgeway, London NW1 7AA, United Kingdom

[◆]Department of Biochemistry and Molecular & Cellular Biology, Georgetown University, Washington, District of Columbia 20007, United States

Supporting Information

ABSTRACT: Alzheimer's disease (AD) is the most common cause of adult dementia. Yet the complete set of molecular changes accompanying this inexorable, neurodegenerative disease remains elusive. Here we adopted an unbiased lipidomics and metabolomics approach to surveying frozen frontal cortex samples from clinically characterized AD patients (n = 21) and age-matched controls (n = 19), revealing marked molecular differences between them. Then, by means of metabolomic pathway analysis, we incorporated the novel molecular information into the known biochemical pathways and compared it with the results of a metabolomics meta-analysis of previously published AD research. We found six metabolic pathways of the central metabolism as well as glycerophospholipid metabolism predominantly altered in AD brains. Using targeted metabolomics approaches and MS imaging, we confirmed a marked dysregulation of mitochondrial aspartate metabolism. The altered metabolic pathways were further integrated with clinical data, showing various degrees of correlation with parameters of dementia and AD pathology. Our study highlights specific, altered biochemical pathways in the brains of individuals with AD compared with those of control subjects, emphasizing dysregulation of mitochondrial aspartate metabolism and supporting future venues of investigation.

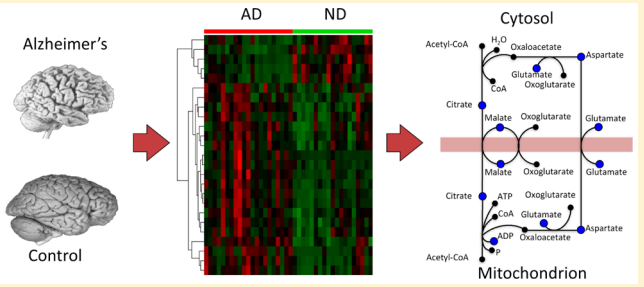

KEYWORDS: *lipidomics, Alzheimer's disease, metabolomics, lipids, metabolic pathways*

INTRODUCTION

Alzheimer's disease (AD) is the most common cause of adult-onset dementia. Rising life expectancy is associated with increased prevalence and incidence of dementia. A recent report estimates that one in every three people born in the United Kingdom in 2015 will suffer from this debilitating mental illness during their lifetime.[1] The need to identify novel molecular targets for AD to use in diagnostics and therapeutics is acute. Although a growing number of clinical research laboratories use mass spectrometry (MS) applications to investigate proteomic changes in AD,[2−6] insufficient effort has been dedicated to studying alterations in levels of small molecules, metabolites, and lipids.[2,7−9] To effectively address any therapeutic challenge in AD, however, requires detailed information about its underlying molecular pathology.

Previous studies by our group and others have examined the profound biochemical alterations in the AD brain.[2,10−18] Most of those studies adopted targeted analytical approaches that, based on prior hypotheses, focused on a particular group of lipids or metabolites, belonging, for example, to a specific metabolic pathway. Changes in selected lipids or metabolites in AD brains, it is speculated, result from a cascade of cellular events involving abnormal β-amyloid protein metabolism, τ

Received: November 3, 2015
Published: December 30, 2015

DOI: 10.1021/acs.jproteome.5b01020
J. Proteome Res. 2016, 15, 608−618

phosphorylation, oxidative stress, mitochondrial or peroxisomal dysfunctions, inflammation, neurotransmitter changes, membrane lipid dysregulation, apoptosis, or changes in other proteins/chemicals.[19,20] According to a targeted analytical approach, however, the specific lipids or metabolites that undergo analysis are selected according to the questions asked, which might hinder the discovery of unexpected metabolic dysregulations in AD brains.

The use of untargeted metabolomics and lipidomics approaches, on the other hand, can offer an unbiased view of the molecular changes occurring in AD brains.[21,22] Untargeted approaches are hypothesis-generating and exploratory in nature, their purpose being to obtain profiles of as many metabolites and lipids as possible in biological samples. By comparing metabolite and lipid profiles, we can thus determine patterns of variations between control and AD subjects, and we can generate novel hypotheses or support old venues of investigations. According to an untargeted analytical approach, features of interest are selected on the basis of statistical analyses and are then identified and eventually quantified by more targeted approaches. Yet most untargeted studies are focused on biomarker discovery and usually provide only a list of individual molecular species that are altered, while failing to highlight the functional connectivity among different biochemical pathways in AD brains.

Recent technological advances in the field of MS and bioinformatics allows us to combine untargeted and targeted analytical approaches in a single analysis to provide simultaneously a bird's-eye view of the interconnected metabolic changes as well as a magnified view of selected biochemical pathways of interest, providing novel opportunities to investigate AD brains. Furthermore, while traditional approaches generally involve processing and extracting the samples before MS analysis, which may alter the chemical composition of the molecules under study, novel analytical approaches such as MS imaging allow determination of the spatial localization of lipids or metabolites in their natural environment. By scanning through tissues, MS imaging allows us to generate topographical maps of molecular distribution in the AD brain.[23,24]

In this study, we used a combination of state-of-the-art untargeted and targeted lipidomics and metabolomics, as well as MS imaging, to profile postmortem brains from AD subjects and nondemented controls. Using innovative biostatistical and bioinformatical approaches, we highlighted specific biochemical pathways altered in AD, which were then correlated with clinical records such as degrees of dementia and pathology. Finally, we compared our results with a meta-analysis of previously published research on AD, supporting venues of investigations in AD research.

EXPERIMENTAL SECTION

Chemicals

All chemicals and polar metabolites used as standards were purchased from Sigma–Aldrich (Seelze, Germany) and were of analytical-grade purity or higher. Lipid standards were purchased from Avanti Polar Lipids (Alabaster, AL) and Cayman Chemicals (Ann Arbor, MI).

Tissue Procurement

From a cohort of 19 control subjects (12:7, males to females) and 21 subjects with AD (9:12, males to females), frozen human samples were obtained from the Banner Sun Health Research Institute (Sun City, AZ) (Table 1). The samples were matched for age: 83.5 ± 6.4 years for the control subjects and 82.4 ± 6.7 years for subjects with AD (mean ± standard deviation, SD). The samples were also matched for postmortem interval: 3.6 ± 1.7 h for control subjects and 3.6 ± 1.4 h for subjects with AD (mean ± SD) (Table 1). AD cases met the criteria of the National Institute on Aging–Reagan Institute for intermediate or high likelihood of Alzheimer's disease. All subjects or, where appropriate, their caregivers provided written, informed consent for the clinical examination as well as for brain donation to the Banner Sun Health Research Institute Brain and Body Donation Program. The protocols and informed consent are approved by the Banner Health Institutional Review Board.

Sample Preparation

Frozen brain samples were rapidly weighed (20 mg) and homogenized in ice-cold methanol (1 vol) containing the following internal standards: arachidonic acid-d_8, cholesterol-d_7, C19:0-cholesteryl ester, trinonadecenoin, 1,2-dimyristoyl-*sn*-glycero-3-phosphoethanolamine, 1,2-dimyristoyl-*sn*-glycero-3-phosphocholine, 1-heptadecenoyl-2-hydroxy-*sn*-glycero-3-phosphocholine, phenylalanine-d_2, succinate-d_4, [$^{13}C_6$]glucose, carnitine-d_9, glutamic acid-d_5, lysine-d_4, alanine-d_4, and [$^{13}C_{10}$,$^{15}N_5$]AMP. Metabolites were extracted by adding chloroform and water (2:1 v/v) and centrifuged at 10000*g* for 10 min at 4 °C. The bottom phases (mostly lipids) were dried under nitrogen, reconstituted in 2-propanol/acetonitrile/water (4:3:1 v/v/v, 0.1 mL) and subjected to liquid chromatography–masss spectrometry (LC–MS) analysis. The upper phases (polar metabolites) were dried under vacuum, reconstituted in water/acetonitrile (1:1 v/v, 0.2 mL), and subjected to LC–MS analysis. A small amount (10 μL) from each sample was pooled, for use as quality controls for LC–MS analyses.

Metabolomic Analyses

Chromatographic separation was achieved by use of an Acquity ultraperformance liquid chromatography (UPLC) system (Waters Corporation, Milford, MA) and hydrophilic-interaction liquid chromatography (HILIC) using a 1.7 μm (2.1 × 150 mm) Acquity amide column (Waters).[25−27] A Synapt G2 mass spectrometer (Waters) was coupled with the UPLC system and operated in data-independent mode (MS^E).[28] Pooled samples were analyzed in high-definition MS^E mode ($HDMS^E$).[23,29] In positive electrospray mode, the capillary and cone voltage were 1.5 kV and 30 V, respectively. The source and desolvation temperatures were 120 and 500 °C, respectively, and the flow rate of desolvation gas was 800 L/h. During MS^E experiments, the collision energy in the trap cell was 4 eV (function 1), and in the transfer cell, it ranged from 15 to 30 eV (function 2).

Samples were analyzed three times by UPLC–HILIC–MS^E, once in positive ionization mode and twice in negative ionization mode, under acidic and basic chromatographic conditions, respectively.[25,30] In positive mode and in negative acidic conditions, mobile phase A was 100% acetonitrile and mobile phase B was 100% H_2O, with both containing 0.1% formic acid. The following elution gradient was used: 0 min, 99% A; 6 min, 40% A; 8 min, 99% A; 10 min, 99% A. In negative-mode basic conditions, mobile phase A contained acetonitrile/sodium bicarbonate, 10 mM (95:5), and mobile phase B contained acetonitrile/sodium bicarbonate, 10 mM (5:95). The following elution gradient was used: 0 min, 99% A; 5 min, 42% A; 6 min, 70% A; 7 min, 99%; 10 min, 99% A. In all

DOI: 10.1021/acs.jproteome.5b01020
J. Proteome Res. 2016, 15, 608–618

conditions, the flow rate was 0.4 mL/min, the column temperature was 45 °C, and the injection volume was 3.5 μL.

Lipidomic Analyses

Lipidomic analyses of the brain samples were performed by use of an ionKey/MS system composed of the Acquity UPLC M-Class, ionKey source, and an iKey CSH C18 130 Å (1.7 μm particle size) 150 μm × 100 mm column (Waters) coupled to a Synapt G2-Si (Waters). Analyses were conducted with both positive and negative electrospray in MS^E mode. Pooled samples were analyzed in high-definition MS^E mode ($HDMS^E$).[23,24,31] The capillary voltage was 2.8 kV and the source temperature was 110 °C. Injections were 0.5 μL in the partial-loop mode, with a column temperature of 55 °C and flow rate of 3 μL/min. Mobile phase A consisted of acetonitrile/water (60:40) with 10 mM ammonium formate + 0.1% formic acid. Mobile phase B consisted of 2-propanol/acetonitrile (90:10) with 10 mM ammonium formate + 0.1% formic acid. The gradient was programmed as follows: 0.0−2.0 min, from 40% to 43% B; 2.0−2.1 min, to 50% B; 2.1−12.0 min, to 99% B; 12.0−12.1 min, to 40% B; and 12.1−14.0 min, at 40% B.

Laser Ablation Electrospray Ionization Mass Spectrometric Imaging

Frozen human brain samples were serially sectioned in a cryostat, to allow alternate microscopic and MS-imaging analyses. Sections were placed on standard microscope slides and kept frozen at −15 °C throughout the analysis using the Peltier cooling stage of laser ablation electrospray ionization (LAESI). Sections were analyzed on a LAESI DP-1000 Direct Ionization System (Protea Bioscience, Morgantown, WV) coupled with a Synapt G2-S mass spectrometer operated in HDMS mode. The electrospray solution for LAESI was methanol/water (50:50 v/v) with 0.1% acetic acid. LAESI parameters consisted of 10 laser pulses/pixel, at 5 Hz and 800 μJ laser energy. Data were collected in both negative- and positive-ion modes with a mass range of m/z 50−1500 for MS scans as well as for ion mobility−MS scans. Identifications were made according to accurate mass and collision cross sections (CCS) values.[29] Selected drift-time regions were extracted by use of DriftScope software (Waters). Ion distribution maps were created for mass values of interest by use of ProteaPlot v2.0.3.8 (Protea Bioscience).

Data Processing and Analysis

Data processing and analysis was conducted by use of Progenesis QI Informatics (Nonlinear Dynamics, Newcastle, U.K.).[29] Each UPLC−MS run was imported as an ion-intensity map, including m/z and retention time. These ion maps were then aligned in the retention-time direction. From the aligned runs, an aggregate run representing the compounds in all samples was used for peak picking. This aggregate was then compared with all runs, to ensure that the same ions are detected in every run. Isotope and adduct deconvolution was applied, to reduce the number of features detected. Data were normalized according to total ion intensity. A combination of analysis of variance (ANOVA) and multivariate statistics, including principal-component analysis (PCA) and orthogonal partial least-squares discriminant analysis (OPLS-DA), identified features most responsible for differences between sample groups. Before multivariate analysis, data were scaled by Pareto and log-transformed. PCA and OPLS-DA were performed with SIMCA-P (Umetrics, Umea, Sweden), Metabolites were identified by database searches against their accurate masses in publicly available databases, including the LIPID MAPS[32] database and the Human Metabolome database (HMDB),[33] as well as by fragmentation patterns, retention times, and CCS values, when available. Pathway analysis, which consisted of enrichment analysis and pathway topological analysis, were conducted with the Metabolomics Pathway Analysis (MetPA) feature within MetaboAnalyst.[34] TargetLynx software (Waters) was used for targeted analysis of selected features with internal standards for each class as previously reported.[25,30] Correlation analysis was performed by MetaboAnalyst.[34] Pearson test (r) was used to measure the correlation.

Metabolite Cluster Enrichment Analysis

Enrichment analysis of changed metabolite classes, subclasses, and LIPID MAPS[32] subclasses was performed according to the methods previously used by Watschinger et al.,[35] with some modifications. Briefly, a distance matrix between metabolite profiles was generated by hierarchical clustering of normalized profiles (Z-scores) and then used to separate the metabolites into six clusters, according to their similarities. For each cluster, HMDB[33] class, HMDB subclass, and LIPID MAPS[32] subclass enrichment analysis was performed separately. Depending on the level on which the enrichment analysis was performed, all annotated IDs from the respective databases were used. For each individual HMDB class, HMDB subclass, and LIPID MAPS subclass, a hypergeometric test based on the counts of significantly altered compounds versus all possible identifications was performed. We selected an ANOVA p-value of 0.01 and a minimum number of three or more compounds per category as significance criteria. Every enrichment analysis was performed separately for the complete data set as well as for all six clusters identified on the basis of profile similarity (as described above).

Metabolomics Pathway Meta-Analysis

The PubMed database was cross-searched (in March 2015) for the term "Alzheimer" and each metabolite present in the HMDB in all fields (i.e., title, abstract, keywords). Information about the human metabolome was downloaded from the HMDB at the Web address www.hmdb.ca/download. Each metabolite entry was saved as an extensible markup language (XML) file called MetaboCard. Each MetaboCard entry contains more than 110 data fields, with two-thirds of the information devoted to chemical and physical data and the remaining third to enzymatic or biochemical data. Many data fields are linked to other databases (KEGG, PubChem, MetaCyc, ChEBI, PDB, UniProt, and GenBank).[33,36,37] R software,[38] running on scripts developed in-house, was used to gain access to the MetaboCard entries, to obtain information about each metabolite and its synonyms, and to query the PubMed database in all fields (i.e., title, abstract, keywords). Because in the literature the same metabolite can be present under different names, each query to PubMed was parsed as follows: "Alzheimer AND (synonym#1 OR synonym#2 OR synonym#3 OR synonym#4)". The functions xmlTreeParse and xmlValue of the R-package XML were used to analyze the output from PubMed and to count the numbers of papers for each query. A metabolite-set enrichment analysis (MSEA) was performed by over-representation analysis (ORA) using the Web tool freely available at the Internet address http://www.msea.ca/MSEA/.

DOI: 10.1021/acs.jproteome.5b01020
J. Proteome Res. 2016, 15, 608−618

RESULTS

Table 1 shows the demographic and neuropathological characteristics of the subjects with AD and the control subjects

Table 1. Demographic and Neuropathological Features of Subjects in This Study[a]

	AD subjects	control subjects
total number	21	19
sex (male/female)	9/12	12/7
age, years	82.4 ± 6.7	83.5 ± 6.4
postmortem interval, hours	3.6 ± 1.4	3.6 ± 1.7
tangle score (Braak and Braak)	V (n = 11); VI (n = 10)	I (n = 2); II (n = 4); III (n = 7); IV (n = 6);
plaque density	frequent (20); Moderate (1)	zero (7); sparse (2); moderate (4); frequent (6)
MMSE score	13.4 ± 7.9	28.0 ± 1.7
BMI	24.7 ± 3.8	25.0 ± 3.9

[a]Plus and minus values are means ± SD. BMI, body-mass index; MMSE, mini-mental status examination.

used in this study. Notably, in order to limit artifacts due to aging or tissue degradation, the groups were closely matched for age and postmortem interval, which on average was kept under 4 h.

Unbiased Metabolomic and Lipidomic Analyses

To extract metabolites and lipids from the same brain tissue samples, we used a biphasic liquid/liquid extraction method. The procedure permitted the extraction of selectively polar metabolites in the aqueous phase while lipids were isolated in the organic phase. We then applied, separately, our untargeted metabolomic and lipidomic workflows to these samples. Additional brain samples were also prepared for MS imaging analyses (Figure 1).

To determine whether the disease induced molecular differences in AD brains, we first used multivariate statistical approaches as an initial step for data visualization. PCA and OPLS-DA showed clear clustering of the control and AD brains for both lipidomic (Figure S1a, Supporting Information) and metabolomic (Figure S1b, Supporting Information) analyses. Integration of lipidomic and metabolomic information showed that 82% of metabolite alterations presented joint variations with lipids, whereas 20% of the lipids evidenced unique variations (Figure S1c, Supporting Information). These observations indicate that AD brains sustained profound molecular changes that affected both lipids and other metabolic pathways in an interconnected fashion.

Enrichment Analyses

To determine the chemical classes of lipids and metabolites altered in AD brains, we performed a hierarchical clustering analysis of all the potential molecular identifications (Figure 2A). Metabolites could be divided into six clusters, according to the distance between their individual profiles (Figure 2). Three of the clusters (1, 3, and 4) were characterized by a significant increase in metabolite levels in AD samples, compared with nondemented (ND) controls (Figure 2a). The remaining three clusters (2, 5, and 6) revealed the opposite effect: higher levels of metabolites in the controls (Figure 2A).

Although the apparent differences between clusters with similar profile changes are small, our enrichment analysis revealed that the clusters have distinct metabolic compositions (Figure 2B,C). The HMDB classification system allowed us to

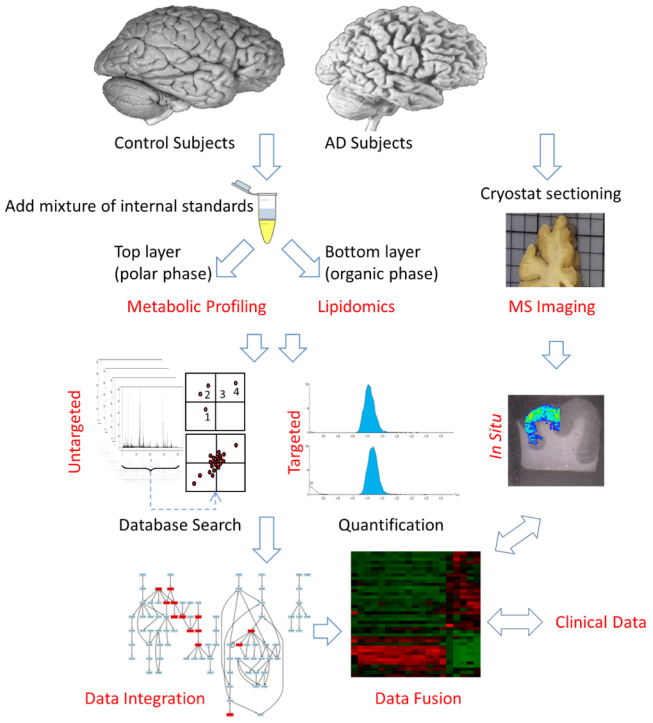

Figure 1. Experimental workflow. Frontal cortex samples from AD subjects (n = 21) and nondemented controls (n = 19) were extracted via a biphasic system ($CHCl_3/CH_3OH/H_2O$, 2:1:1 v/v/v). Top layer was analyzed by a metabolomics approach for polar metabolites; bottom layer was analyzed by a lipidomics approach for lipids. Initial discovery data were further investigated by targeted metabolic-profiling approaches and MS imaging. The results were then fused and integrated with clinical parameters.

differentiate metabolites according to their kingdom, superclass, class, and subclass (Figure 2B). The LIPID MAPS classification system provided additional information. Located one layer below the HMDB subclass information, the LIPID MAPS subclass information, with an associated LIPID MAPS ID, was also included in the analysis for metabolites (Figure 2C). This analysis indicated that the lipid class of glycerophospholipids—in particular, phosphatidylcholines and phosphatidylethanolamines—appeared to be mostly altered in AD brains, compared with control brains, a finding cited in previous reports.[10,20,39−47] It is important to note that the same class of metabolites, such as glycerophospholipids, showed an increase in AD in clusters 1−3 but a decrease in clusters 4 and 5 (Figure 2B), which indicates differential regulation of lipid species within the same subclass (Figure 2C). Changes in lipid composition may profoundly affect membrane structure, transmembrane signaling, and cell-to-cell communication in the brain, and they may thus underlie an important aspect of AD pathology. Further studies will aim to validate such lipid variations and their relationship to AD.

Alterations in Metabolic Pathways

To determine the biochemical pathways mostly affected in AD brains, we identified and monitored by a targeted approach[25] a subset of polar metabolite that was shown to discriminate between brains from AD patients and those from ND controls (Figure 3a,b). Metabolites were identified from an in-house database[24,25,29] and, where standards were not available, by comparing exact mass and fragmentation spectra information with online databases. Metabolomics pathway analysis indicated

DOI: 10.1021/acs.jproteome.5b01020
J. Proteome Res. 2016, 15, 608−618

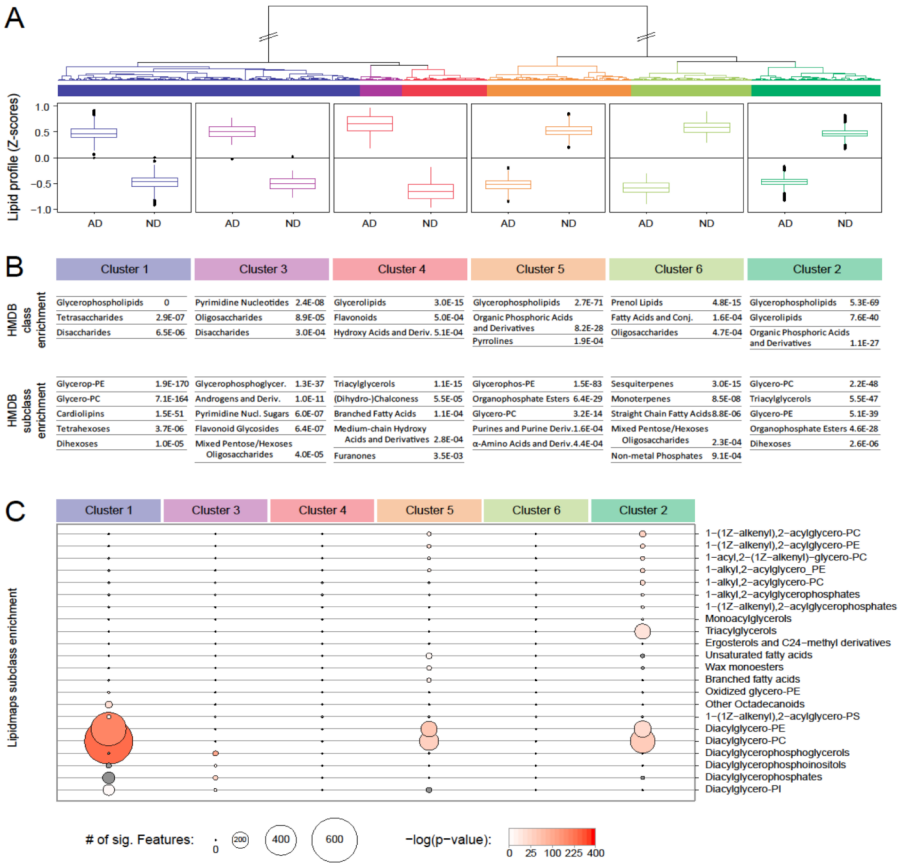

Figure 2. Metabolite cluster and enrichment analysis of molecular species affected by AD. (A) Unsupervised hierarchical clustering analysis of all the potential molecular identifications according to their coregulation in AD brains. The clustered profiles were divided into six different groups with distinctive behavior. Metabolite and lipid concentration changes are shown in the respective groups. Each box is calculated from all lipids belonging to the respective group, each with peak-area data from five biological replicates. *Z* scores were determined according to the mean and SD of all data for the respective metabolite. (B) Enrichment analysis obtained by use of the HMDB classification system. (C) Lipid subclass enrichment analysis obtained by use of the LIPID MAPS classification system. Only significantly enriched subclasses for AGMO modulation are shown (*P*-value of enrichment <0.001). Circle size represents the number of lipid species matching the respective subclass. Enrichment *P*-values are indicated by the intensity of coloration of the circles.

six metabolic pathways affected during AD (Figure 3c,d and Table 2). In particular, alanine, aspartate, and glutamate metabolism proved one of the most affected pathways in the frontal cortices of subjects with AD, compared with those of nondemented control subjects (Figure 3c,d and Table 2).

A significant dysregulation of aspartate and glutamate metabolism was also confirmed by the MS imaging experiment (Figure 4b). Alterations of metabolites such as aspartate, glutamate, citrate, and malate (Figure 4a) as well as accumulation of *N*-acetylaspartate (NAA) (Figure 4b) and pyruvate, serine, and lactate (Figure S2, Supporting Information), in the frontal cortex samples of the AD subjects suggest that the transport mechanism between mitochondria and cytosol might be impaired in AD brains (Figure 4c).

To determine the clinical significance of these metabolomic findings, we created scores indicative of the levels of metabolites belonging to the six metabolic pathways (Table 2) and correlated them with parameters of dementia and AD pathology (Figure 3b,d). For each pathway a PLS model was built considering the metabolite concentrations as *X* and the metadata as *y*. A permutation test on *y* and a stability test based on Monte Carlo sampling and PLS VIP-based were performed to check overfitting. The set of metabolites detected by stability test was used to calculate $Q^2_{CV,7\text{-fold}}$ (i.e., R^2 calculated by 7-fold, full, cross-validation). Robust models for all pathways were found for AD, with the alanine, aspartate, and glutamate pathway having the strongest correlation. No associations with age, postmortem interval (PMI), body mass index (BMI), and gender (Figure 3b,d) were found, with the only exception being a minor association between pathway 5 and gender (Figure 3 d). All the pathways were strongly associated with pathological hallmarks of AD, such as tangles, while a smaller association was found with plaques. One of the most promising models for explaining cognitive status as measured by mini-mental state examination (MMSE) was found for metabolites of the alanine, aspartate, and glutamate pathway.

An in-depth analysis of the alanine, aspartate, and glutamate pathway revealed that the levels of aspartic acid and succinic acid positively correlated with MMSE, whereas the levels of pyruvic acid, glutamine, and NAA negatively correlated with MMSE (Figure S3, Supporting Information). Levels of alanine, asparagine, and glutamic acid showed only a weak correlation with the clinical data (Figure S3, Supporting Information).

Literature Comparison

To compare our results with the literature, we performed a metabolomics meta-analysis of the previously published AD literature in PubMed. We cross-searched the terms "Alzheimer" and the complete list of metabolites and their synonyms, as

DOI: 10.1021/acs.jproteome.5b01020
J. Proteome Res. 2016, 15, 608−618

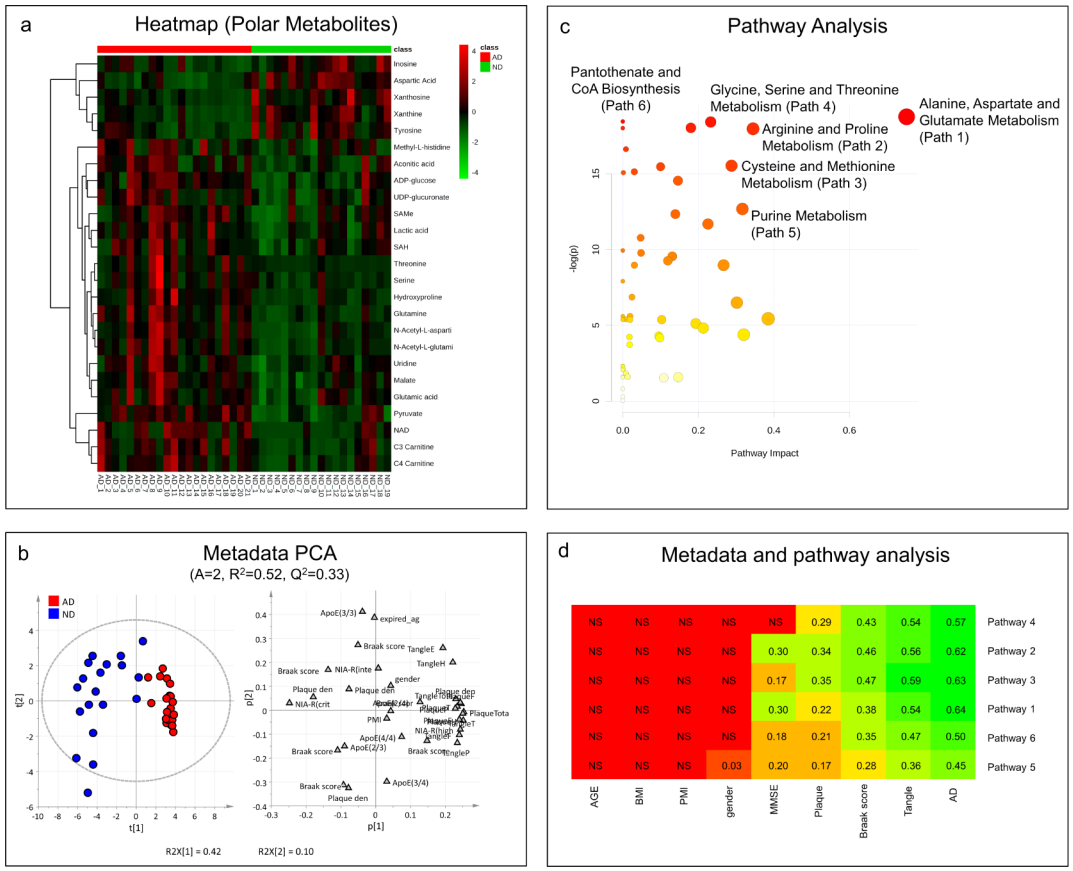

Figure 3. Integration of metabolomics and clinical information. (a) Heat map of selected polar metabolites. (b) Principal component analysis performed on clinical information. (c) Pathway analysis performed on metabolomics results. (d) Integration of pathway analysis results with clinical information. The heat map shows the relationships between clinical data and pathways. Pathways and metadata are ordered according to hierarchical cluster analysis, to simplify interpretation of the map. Metadata close to each other have a similar profile with respect to relationships with the pathways, while pathways close to each other show similar relationships with respect to the metadata; here "relationships" means linear relationships between the concentrations of the metabolites included in the pathway and the metadata on the basis of PLS regression. The heat map was colored according to $Q^2_{CV,7\text{-fold}}$. NS means no significant PLS regression model ($Q^2_{CV,7\text{-fold}}$ p-value > 0.05).

reported in HMDB (41 514 entries).[33] We then used the number of publications as an index of correlation between AD and the metabolite. A metabolite-set enrichment analysis[37] helped identify patterns of metabolites most studied in AD research. It showed the aspartate and glutamate pathway as historically one of the most studied, agreeing with the outcome of our metabolomics investigation (Figure S4, Supporting Information).

DISCUSSION

In this study we used a combination of innovative analytical approaches to conduct an unbiased metabolomics and lipidomics investigation of the biochemical pathways that are affected in AD brains.

As for all metabolomics and lipidomics analyses, study design, such as sample size, postmortem interval, and genotype (e.g., ApoE), as well as standard operating procedures, such as sample preparation, can affect results. Our study had multiple key features in terms of the analytical aspects that should be taken into consideration. First, our cohort size was of 21 AD subjects and 19 nondemented controls; groups were matched by age and postmortem interval, and frontal cortices were selected as region of the brain. Second, in order to limit artifacts due to sample degradation, our criteria for subject selection required a postmortem interval average of less than 4 h, which is remarkably short for postmortem brains. Third, to further limit artifacts due to enzymatic reactions and oxidation, brain samples were weighed while still frozen and then they were quenched with ice-cold methanol. Liquid/liquid extraction allowed us to separate hydrophilic from hydrophobic compounds in a single procedure, and MS imaging was also used to support and confirm traditional analyses while avoiding the process of extracting the samples. Finally, using data-independent acquisition mode, we obviated the need to analyze the sample in untargeted MS mode and then rerun the same sample in targeted MS/MS mode, but instead we automatically acquired the fragmentation data from each precursor ion.[48] The simultaneous generation of high-resolution, full-scan, and fragmentation spectra served as a repository of biological information that was reused after statistical analyses to semiquantify selected biochemical pathways. This approach allowed us to combine untargeted and targeted analysis, maximizing the identification of compounds and biochemical pathways in a single analytical run.

Our study uncovered significant alterations in key mitochondrial metabolites, which correlated with symptoms of dementia and AD pathology. Notably, as highlighted from our literature meta-analysis, previous research on AD largely focused on targeted metabolites of the alanine, aspartate, and glutamate metabolism, often missing a bird's-eye view of the underlying

DOI: 10.1021/acs.jproteome.5b01020
J. Proteome Res. 2016, 15, 608−618

Table 2. List of Most Affected Pathways and Their Metabolites in Human Frontal Cortex of AD Subjects Compared to ND Control Subjects[a]

HMDB ID	metabolite	AD	ND	*t*-test *p*-value
	Path 1: Alanine, Aspartate, and Glutamate Metabolism ($p = 7.19 \times 10^{-9}$)			
HMDB00812	acetylaspartic acid	1.01 ± 0.44	0.57 ± 0.21	2.47×10^{-4}
HMDB00191	aspartic acid	1.50 ± 0.78	3.37 ± 1.33	2.67×10^{-6}
HMDB00161	alanine	5.95 ± 1.68	5.28 ± 1.07	1.45×10^{-1}
HMDB00168	asparagine	0.15 ± 0.07	0.20 ± 0.09	1.07×10^{-1}
HMDB00243	pyruvate	0.09 ± 0.03	0.05 ± 0.03	6.11×10^{-5}
HMDB00148	glutamic acid	24.43 ± 8.58	18.31 ± 7.06	1.92×10^{-2}
HMDB00641	glutamine	43.09 ± 24.72	16.92 ± 10.70	1.28×10^{-4}
HMDB00254	succinic acid	0.20 ± 0.07	0.21 ± 0.10	5.47×10^{-1}
	Path 2: Arginine and Proline Metabolism ($p = 1.58 \times 10^{-8}$)			
HMDB00191	aspartic acid	1.50 ± 0.78	3.37 ± 1.33	2.67×10^{-6}
HMDB00641	glutamine	43.09 ± 24.72	16.92 ± 10.70	1.28×10^{-4}
HMDB00148	glutamic acid	24.43 ± 8.58	18.31 ± 7.06	1.92×10^{-2}
HMDB00517	arginine	12.92 ± 6.00	10.34 ± 3.81	1.17×10^{-1}
HMDB00162	proline	0.17 ± 0.08	0.13 ± 0.06	6.69×10^{-2}
HMDB01185	SAMe	2.03 ± 0.80	1.38 ± 0.83	1.69×10^{-2}
HMDB00725	hydroxyproline	3.21 ± 2.02	1.42 ± 0.85	9.91×10^{-4}
HMDB00243	pyruvate	0.09 ± 0.03	0.05 ± 0.03	6.11×10^{-5}
HMDB01138	acetylglutamic acid	17.77 ± 8.12	9.81 ± 3.66	3.52×10^{-4}
	Path 3: Cysteine and Methionine Metabolism ($p = 1.81 \times 10^{-7}$)			
HMDB00191	aspartic acid	1.50 ± 0.78	3.37 ± 1.33	2.67×10^{-6}
HMDB00187	serine	2.67 ± 1.61	1.54 ± 0.66	7.31×10^{-3}
HMDB00192	cystine	0.197 ± 0.200	0.20 ± 0.20	9.64×10^{-1}
HMDB00161	alanine	5.95 ± 1.68	5.28 ± 1.07	1.45×10^{-1}
HMDB00696	methionine	0.69 ± 0.24	0.58 ± 0.26	1.59×10^{-1}
HMDB00939	SAH	0.82 ± 0.29	0.62 ± 0.22	2.26×10^{-2}
HMDB01185	SAMe	2.03 ± 0.80	1.38 ± 0.83	1.69×10^{-2}
HMDB00243	pyruvate	0.09 ± 0.03	0.05 ± 0.03	6.11×10^{-5}
	Path 4: Glycine, Serine, and Threonine Metabolism ($p = 1.01 \times 10^{-8}$)			
HMDB00191	aspartic acid	1.50 ± 0.78	3.37 ± 1.33	2.67×10^{-6}
HMDB00167	threonine	1.52 ± 1.70	0.31 ± 0.21	3.86×10^{-3}
HMDB00187	serine	2.67 ± 1.61	1.54 ± 0.66	7.31×10^{-3}
HMDB00097	choline	0.59 ± 0.26	0.41 ± 0.24	2.73×10^{-2}
HMDB00929	tryptophan	0.12 ± 0.06	0.10 ± 0.04	3.29×10^{-1}
HMDB00243	pyruvate	0.09 ± 0.03	0.05 ± 0.03	6.11×10^{-5}
	Path 5: Purine Metabolism ($p = 3.13 \times 10^{-6}$)			
HMDB00618	pentose 5-phosphate	0.011 ± 0.005	0.009 ± 0.005	2.87×10^{-1}
HMDB01178	ADP-ribose	0.09 ± 0.07	0.06 ± 0.06	1.52×10^{-1}
HMDB00641	glutamine	43.09 ± 24.72	16.92 ± 10.70	1.28×10^{-4}
HMDB01341	ADP	0.016 ± 0.013	0.010 ± 0.010	1.45×10^{-1}
HMDB00045	AMP	0.32 ± 0.26	0.19 ± 0.22	8.95×10^{-2}
HMDB01397	GMP	0.07 ± 0.04	0.06 ± 0.05	2.97×10^{-1}
HMDB00133	guanosine	2.35 ± 1.84	2.35 ± 2.04	9.99×10^{-1}
HMDB00175	IMP	0.02 ± 0.01	0.01 ± 0.01	2.70×10^{-2}
HMDB00289	uric acid	0.80 ± 0.43	1.10 ± 0.65	8.90×10^{-2}
HMDB00292	xanthine	1.09 ± 0.47	2.29 ± 1.08	4.10×10^{-5}
HMDB00299	xanthosine	0.09 ± 0.04	0.20 ± 0.13	9.03×10^{-4}
HMDB00157	hypoxanthine	25.91 ± 9.08	22.68 ± 9.34	2.74×10^{-1}
HMDB00195	inosine	23.76 ± 11.38	36.80 ± 17.68	7.95×10^{-3}
	Path 6: Pantothenate and CoA Biosynthesis ($p = 1.49 \times 10^{-08}$)			
HMDB00191	aspartic acid	1.50 ± 0.78	3.37 ± 1.33	2.67×10^{-6}
HMDB00243	pyruvate	0.09 ± 0.03	0.05 ± 0.03	6.11×10^{-5}
HMDB00883	valine	0.09 ± 0.03	0.08 ± 0.03	5.21×10^{-1}
HMDB00210	pantothenic acid	2.19 ± 2.18	1.82 ± 0.61	4.77×10^{-1}

[a]Values are expressed as means ± SD of normalized MS intensity. HMDB, Human Metabolome Database.

biochemical alterations and their functional metabolic connectivity. Our metabolomic approach provided a comprehensive view of key metabolites of this pathway, pointing to a specific mitochondrial dysfunction in AD brains, which affects processes involved in the transport of metabolites between mitochondria and cytosol.

DOI: 10.1021/acs.jproteome.5b01020
J. Proteome Res. 2016, 15, 608−618

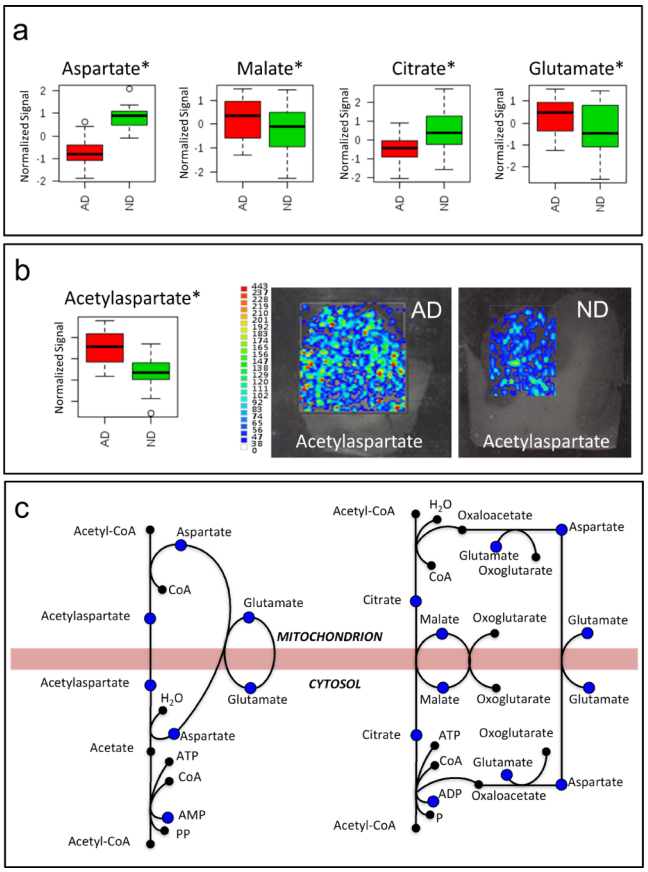

Figure 4. Mitochondrial shuttles. (a) Bar charts of aspartate, malate, citrate, and glutamate obtained from normalized signals in AD (red) and ND control subjects (green). (b) Bar chart of *N*-acetylaspartate (NAA) obtained from normalized signals in AD (red) and control subjects (green) and MS imaging of AD and control subjects brain sections. (c) Mitochondrial shuttles and metabolites quantified in this experiment (blue dots). *$p < 0.05$ (t test). Targeted data used for bar charts were normalized by mean centering, scaled by unit variance, and log-transformed.

Acetyl-CoA can be transported into mitochondria by means of two main shuttles after conversion into either NAA or citrate (Figure 4c). In the first mitochondrial shuttle, NAA is transported into the mitochondria, then converted to acetate by aspartoylacylase, and finally converted back to acetyl-CoA by acetyl-CoA synthetase (Figure 4c). The observation that levels of key metabolites in this process (i.e., NAA, aspartate, and glutamate) are altered in AD and correlated with dementia and pathology suggests that this transport mechanism is affected in AD (Figure 4). In the second mitochondrial shuttle, citrate is transported into the mitochondria and then converted back into acetyl-CoA by ATP-citrate lyase. The observation that levels of key metabolites in this process (i.e., citrate, malate, glutamate, and aspartate) were significantly changed in AD supports an impairment in the transport mechanism. The fact that key metabolites in both mitochondrial shuttles are altered could reflect a more general mitochondrial dysfunction in AD brains.

The role of mitochondria as regulators of brain energy metabolism makes it crucial to neuronal cell survival or death. Growing evidence indicates that mitochondrial dysfunction is an early event during the progression of AD and one of the key intracellular mechanisms associated with the pathogenesis of this disease.[49−52] Recent findings demonstrated that α-ketoglutarate dehydrogenase complex regulates mitochondrial metabolism through post-translational modification of other enzymes in mitochondria[53] and that AD patients have decreased activity of this enzyme.[54]

Our observations agree with a recent report that was ^{1}H NMR-based.[55] Altered concentrations of brain NAA, as measured by magnetic resonance (MR), have been commonly associated with neurotoxicity, and its levels have been used to assess in vivo neuronal loss and neurodegeneration in AD.[56−58] However, NAA concentration in the brain varies according to the brain region investigated. Indeed, it has been shown that the concentration of NAA selectively decreases in specific brain areas such as the hippocampus and amygdala but not in the frontal cortex.[59]

We cannot exclude that the levels of NAA and other metabolites are a consequence of dietary regimens or pharmacological treatments of the AD subjects. Previous evidence indicates, for example, that levels of NAA increase during cholinergic treatment in AD[60,61] and could be reversed after other therapeutic interventions.[62,63] Further investigations are needed to better understand the role of mitochondrial aspartate metabolism in AD.

CONCLUSIONS

AD is a neurodegenerative disorder characterized by the loss of cognitive abilities and the appearance of pathological hallmarks in the brain, such as extraneuronal plaques and neurofibrillary tangles. In this study, we used an innovative analytical approach based on a combination of untargeted and targeted lipidomic and metabolomics, as well as MS imaging, to investigate metabolic alterations occurring in the AD brain. We explored the biochemical significance of observed metabolic alterations according to known metabolic pathways. We then used novel bioinformatics and biostatistical approaches to integrate the novel acquired metabolic knowledge of AD brains with clinical records and literature metadata. Most notably, we uncovered a significant dysregulation in mitochondrial aspartate metabolism in the AD brain, which correlated with dementia and AD pathology. As such, our study provides a solid rationale for future pharmacological or metabolic interventions and other functional experiments aimed to better understand the role played by mitochondrial aspartate metabolism in the etiology and progression of the cognitive impairment and pathological hallmarks associated with AD. Our study also suggests novel venues of investigation for biomarker discovery in peripheral tissues, such as blood, related to the metabolic changes that we observed in AD brains.

ASSOCIATED CONTENT

Supporting Information

The Supporting Information is available free of charge on the ACS Publications website at DOI: 10.1021/acs.jproteome.5b01020.

Four figures showing PCA and OPLS-DA analysis of untargeted lipidomics and metabolomics results; bar charts of lactate, pyruvate, and serine; PLS model with metabolite concentrations as X and metadata as y; and pathway and enrichment analysis of metabolites most studied in AD research (PDF)

DOI: 10.1021/acs.jproteome.5b01020
J. Proteome Res. 2016, 15, 608−618

AUTHOR INFORMATION

Corresponding Author

*E-mail giuseppe_astarita@waters.com; phone 5084822452.

Notes

The authors declare no competing financial interest.

ACKNOWLEDGMENTS

This work was partially funded by the Alzheimer's Association (NIRG-11-203674 to G.A.), the Wellcome Trust (RG 093735/Z/10/Z to M.R.), and the ERC (Starting Grant 260809 to M.R.). We are indebted to Drs. Thomas Beach and Geidy Serrano for their support and also to the Sun Health Research Institute Brain and Body Donation Program of Sun City, Arizona, for providing human biological materials. Finally, we thank Manuela Magnusdottir for her technical assistance. M.R. is a Wellcome Trust Research Career Development and Wellcome−Beit Prize fellow.

REFERENCES

(1) Lewis, F. *Estimation of future cases of dementia from those born in 2015*; Office of Health Economics: London, 2015; https://www.ohe.org/publications/estimation-future-cases-dementia-those-born-2015.

(2) Fonteh, A. N.; Harrington, R. J.; Huhmer, A. F.; Biringer, R. G.; Riggins, J. N.; Harrington, M. G. Identification of disease markers in human cerebrospinal fluid using lipidomic and proteomic methods. *Dis. Markers* **2006**, *22* (1−2), 39−64.

(3) Castano, E. M.; Roher, A. E.; Esh, C. L.; Kokjohn, T. A.; Beach, T. Comparative proteomics of cerebrospinal fluid in neuropathologically-confirmed Alzheimer's disease and non-demented elderly subjects. *Neurol. Res.* **2006**, *28* (2), 155−163.

(4) Huang, J. T.; Leweke, F. M.; Oxley, D.; Wang, L.; Harris, N.; Koethe, D.; Gerth, C. W.; Nolden, B. M.; Gross, S.; Schreiber, D.; Reed, B.; Bahn, S. Disease Biomarkers in Cerebrospinal Fluid of Patients with First-Onset Psychosis. *PLoS Med.* **2006**, *3* (11), No. e428.

(5) Zhang, J.; Goodlett, D. R.; Quinn, J. F.; Peskind, E.; Kaye, J. A.; Zhou, Y.; Pan, C.; Yi, E.; Eng, J.; Wang, Q.; Aebersold, R. H.; Montine, T. J. Quantitative proteomics of cerebrospinal fluid from patients with Alzheimer disease. *J. Alzheimers Dis.* **2005**, *7* (2), 125−133 (see also discussion, pp 173−180 in this issue)..

(6) Montine, T. J.; Woltjer, R. L.; Pan, C.; Montine, K. S.; Zhang, J. Liquid chromatography with tandem mass spectrometry-based proteomic discovery in aging and Alzheimer's disease. *NeuroRx* **2006**, *3* (3), 336−343.

(7) Ackermann, B. L.; Hale, J. E.; Duffin, K. L. The role of mass spectrometry in biomarker discovery and measurement. *Curr. Drug Metab.* **2006**, *7* (5), 525−539.

(8) Chace, D. H. Mass spectrometry in the clinical laboratory. *Chem. Rev.* **2001**, *101* (2), 445−477.

(9) Mapstone, M.; Cheema, A. K.; Fiandaca, M. S.; Zhong, X.; Mhyre, T. R.; MacArthur, L. H.; Hall, W. J.; Fisher, S. G.; Peterson, D. R.; Haley, J. M.; Nazar, M. D.; Rich, S. A.; Berlau, D. J.; Peltz, C. B.; Tan, M. T.; Kawas, C. H.; Federoff, H. J. Plasma phospholipids identify antecedent memory impairment in older adults. *Nat. Med.* **2014**, *20* (4), 415−418.

(10) Lukiw, W. J.; Cui, J.-G.; Marcheselli, V. L.; Bodker, M.; Botkjaer, A.; Gotlinger, K.; Serhan, C. N.; Bazan, N. G. A role for docosahexaenoic acid-derived neuroprotectin D1 in neural cell survival and Alzheimer disease. *J. Clin. Invest.* **2005**, *115* (10), 2774−2783.

(11) Cutler, R. G.; Kelly, J.; Storie, K.; Pedersen, W. A.; Tammara, A.; Hatanpaa, K.; Troncoso, J. C.; Mattson, M. P. Involvement of oxidative stress-induced abnormalities in ceramide and cholesterol metabolism in brain aging and Alzheimer's disease. *Proc. Natl. Acad. Sci. U.S.A.* **2004**, *101* (7), 2070−2075.

(12) Puglielli, L.; Tanzi, R. E.; Kovacs, D. M. Alzheimer's disease: the cholesterol connection. *Nat. Neurosci.* **2003**, *6* (4), 345−351.

(13) Pappolla, M. A.; Smith, M. A.; Bryant-Thomas, T.; Bazan, N.; Petanceska, S.; Perry, G.; Thal, L. J.; Sano, M.; Refolo, L. M. Cholesterol, oxidative stress, and Alzheimer's disease: expanding the horizons of pathogenesis. *Free Radical Biol. Med.* **2002**, *33* (2), 173−181.

(14) Farooqui, A. A.; Rapoport, S. I.; Horrocks, L. A. Membrane phospholipid alterations in Alzheimer's disease: deficiency of ethanolamine plasmalogens. *Neurochem. Res.* **1997**, *22* (4), 523−527.

(15) Wells, K.; Farooqui, A. A.; Liss, L.; Horrocks, L. A. Neural membrane phospholipids in Alzheimer disease. *Neurochem. Res.* **1995**, *20* (11), 1329−1333.

(16) Farooqui, A. A.; Liss, L.; Horrocks, L. A. Neurochemical aspects of Alzheimer's disease: involvement of membrane phospholipids. *Metab. Brain Dis.* **1988**, *3* (1), 19−35.

(17) Astarita, G.; Jung, K. M.; Vasilevko, V.; Dipatrizio, N. V.; Martin, S. K.; Cribbs, D. H.; Head, E.; Cotman, C. W.; Piomelli, D. Elevated stearoyl-CoA desaturase in brains of patients with Alzheimer's disease. *PLoS One* **2011**, *6* (10), No. e24777.

(18) Astarita, G.; Jung, K. M.; Berchtold, N. C.; Nguyen, V. Q.; Gillen, D. L.; Head, E.; Cotman, C. W.; Piomelli, D. Deficient liver biosynthesis of docosahexaenoic acid correlates with cognitive impairment in Alzheimer's disease. *PLoS One* **2010**, *5* (9), No. e12538.

(19) Pettegrew, J. W.; Panchalingam, K.; Hamilton, R. L.; McClure, R. J. Brain membrane phospholipid alterations in Alzheimer's disease. *Neurochem. Res.* **2001**, *26* (7), 771−782.

(20) Prasad, M. R.; Lovell, M. A.; Yatin, M.; Dhillon, H.; Markesbery, W. R. Regional membrane phospholipid alterations in Alzheimer's disease. *Neurochem. Res.* **1998**, *23* (1), 81−88.

(21) Inoue, K.; Tsutsui, H.; Akatsu, H.; Hashizume, Y.; Matsukawa, N.; Yamamoto, T.; Toyo'oka, T. Metabolic profiling of Alzheimer's disease brains. *Sci. Rep.* **2013**, *3*, No. 2364.

(22) Graham, S. F.; Chevallier, O. P.; Roberts, D.; Holscher, C.; Elliott, C. T.; Green, B. D. Investigation of the human brain metabolome to identify potential markers for early diagnosis and therapeutic targets of Alzheimer's disease. *Anal. Chem.* **2013**, *85* (3), 1803−1811.

(23) Paglia, G.; Kliman, M.; Claude, E.; Geromanos, S.; Astarita, G. Applications of ion-mobility mass spectrometry for lipid analysis. *Anal. Bioanal. Chem.* **2015**, *407* (17), 4995−5007.

(24) Paglia, G.; Angel, P.; Williams, J. P.; Richardson, K.; Olivos, H. J.; Thompson, J. W.; Menikarachchi, L.; Lai, S.; Walsh, C.; Moseley, A.; Plumb, R. S.; Grant, D. F.; Palsson, B. O.; Langridge, J.; Geromanos, S.; Astarita, G. Ion-Mobility-Derived Collision Cross Section as an Additional Measure for Lipid Fingerprinting and Identification. *Anal. Chem.* **2015**, *87* (2), 1137−1144.

(25) Paglia, G.; Sigurjonsson, O. E.; Rolfsson, O.; Valgeirsdottir, S.; Hansen, M. B.; Brynjolfsson, S.; Gudmundsson, S.; Palsson, B. O. Comprehensive metabolomic study of platelets reveals the expression of discrete metabolic phenotypes during storage. *Transfusion* **2014**, *54* (11), 2911−2923.

(26) Paglia, G.; Magnusdottir, M.; Thorlacius, S.; Sigurjonsson, O. E.; Guethmundsson, S.; Palsson, B. O.; Thiele, I. Intracellular metabolite profiling of platelets: evaluation of extraction processes and chromatographic strategies. *J. Chromatogr. B: Anal. Technol. Biomed. Life Sci.* **2012**, *898*, 111−120.

(27) Paglia, G.; Hrafnsdottir, S.; Magnusdottir, M.; Fleming, R. M.; Thorlacius, S.; Palsson, B. O.; Thiele, I. Monitoring metabolites consumption and secretion in cultured cells using ultra-performance liquid chromatography quadrupole-time of flight mass spectrometry (UPLC-Q-ToF-MS). *Anal. Bioanal. Chem.* **2012**, *402* (3), 1183−1198.

(28) Fu, W.; Magnusdottir, M.; Brynjolfson, S.; Palsson, B. O.; Paglia, G. UPLC-UV-MS(E) analysis for quantification and identification of major carotenoid and chlorophyll species in algae. *Anal. Bioanal. Chem.* **2012**, *404* (10), 3145−3154.

(29) Paglia, G.; Williams, J. P.; Menikarachchi, L.; Thompson, J. W.; Tyldesley-Worster, R.; Halldorsson, S.; Rolfsson, O.; Moseley, A.; Grant, D.; Langridge, J.; Palsson, B. O.; Astarita, G. Ion mobility derived collision cross sections to support metabolomics applications. *Anal. Chem.* **2014**, *86* (8), 3985−3993.

DOI: 10.1021/acs.jproteome.5b01020
J. Proteome Res. 2016, 15, 608−618

(30) Paglia, G.; Sigurjonsson, O. E.; Rolfsson, O.; Hansen, M. B.; Brynjolfsson, S.; Gudmundsson, S.; Palsson, B. O. Metabolomic analysis of platelets during storage: a comparison between apheresis- and buffy coat-derived platelet concentrates. *Transfusion* **2015**, *55* (2), 301−313.
(31) Pacini, T.; Fu, W.; Gudmundsson, S.; Chiaravalle, A. E.; Brynjolfson, S.; Palsson, B. O.; Astarita, G.; Paglia, G. Multidimensional analytical approach based on UHPLC-UV-ion mobility-MS for the screening of natural pigments. *Anal. Chem.* **2015**, *87* (5), 2593−2599.
(32) Fahy, E.; Subramaniam, S.; Murphy, R. C.; Nishijima, M.; Raetz, C. R. H.; Shimizu, T.; Spener, F.; van Meer, G.; Wakelam, M. J. O.; Dennis, E. A. Update of the LIPID MAPS comprehensive classification system for lipids. *J. Lipid Res.* **2008**, *50*, S9−S14.
(33) Wishart, D. S.; Jewison, T.; Guo, A. C.; Wilson, M.; Knox, C.; Liu, Y.; Djoumbou, Y.; Mandal, R.; Aziat, F.; Dong, E.; Bouatra, S.; Sinelnikov, I.; Arndt, D.; Xia, J.; Liu, P.; Yallou, F.; Bjorndahl, T.; Perez-Pineiro, R.; Eisner, R.; Allen, F.; Neveu, V.; Greiner, R.; Scalbert, A. HMDB 3.0–The Human Metabolome Database in 2013. *Nucleic Acids Res.* **2013**, *41*, D801−D807 (Database issue).
(34) Xia, J.; Sinelnikov, I. V.; Han, B.; Wishart, D. S. MetaboAnalyst 3.0-making metabolomics more meaningful. *Nucleic Acids Res.* **2015**, *43* (W1), W251−W257.
(35) Watschinger, K.; Keller, M. A.; McNeill, E.; Alam, M. T.; Lai, S.; Sailer, S.; Rauch, V.; Patel, J.; Hermetter, A.; Golderer, G.; Geley, S.; Werner-Felmayer, G.; Plumb, R. S.; Astarita, G.; Ralser, M.; Channon, K. M.; Werner, E. R. Tetrahydrobiopterin and alkylglycerol monooxygenase substantially alter the murine macrophage lipidome. *Proc. Natl. Acad. Sci. U.S.A.* **2015**, *112* (8), 2431−2436.
(36) Liesenfeld, D. B.; Habermann, N.; Owen, R. W.; Scalbert, A.; Ulrich, C. M. Review of mass spectrometry-based metabolomics in cancer research. *Cancer Epidemiol., Biomarkers Prev.* **2013**, *22* (12), 2182−2201.
(37) Xia, J.; Wishart, D. S. MSEA: a web-based tool to identify biologically meaningful patterns in quantitative metabolomic data. *Nucleic Acids Res.* **2010**, *38*, W71−W77 (Web Server issue).
(38) Ihaka, R. R: Past and future history. In *Dimension Reduction, Computational Complexity and Information: Proceedings of the 30th Symposium on the Interface, Minneapolis, Minnesota, May 13−16, 1998*; Computing Science and Statistics, Vol. *30*; Interface Foundation of North America, 1998; pp 392−396.
(39) Brooksbank, B. W.; Martinez, M. Lipid abnormalities in the brain in adult Down's syndrome and Alzheimer's disease. *Mol. Chem. Neuropathol.* **1989**, *11* (3), 157−185.
(40) Soderberg, M.; Edlund, C.; Kristensson, K.; Dallner, G. Fatty acid composition of brain phospholipids in aging and in Alzheimer's disease. *Lipids* **1991**, *26* (6), 421−425.
(41) Guan, Z.; Wang, Y.; Cairns, N. J.; Lantos, P. L.; Dallner, G.; Sindelar, P. J. Decrease and structural modifications of phosphatidylethanolamine plasmalogen in the brain with Alzheimer disease. *J. Neuropathol. Exp. Neurol.* **1999**, *58* (7), 740−747.
(42) Skinner, E. R.; Watt, C.; Besson, J. A.; Best, P. V. Differences in the fatty acid composition of the grey and white matter of different regions of the brains of patients with Alzheimer's disease and control subjects. *Brain* **1993**, *116* (3), 717−725.
(43) Corrigan, F. M.; Horrobin, D. F.; Skinner, E. R.; Besson, J. A.; Cooper, M. B. Abnormal content of n-6 and n-3 long-chain unsaturated fatty acids in the phosphoglycerides and cholesterol esters of parahippocampal cortex from Alzheimer's disease patients and its relationship to acetyl CoA content. *Int. J. Biochem. Cell Biol.* **1998**, *30* (2), 197−207.
(44) Fraser, T.; Tayler, H.; Love, S. Fatty acid composition of frontal, temporal and parietal neocortex in the normal human brain and in Alzheimer's disease. *Neurochem. Res.* **2010**, *35* (3), 503−513.
(45) Cunnane, S. C.; Plourde, M.; Pifferi, F.; Begin, M.; Feart, C.; Barberger-Gateau, P. Fish, docosahexaenoic acid and Alzheimer's disease. *Prog. Lipid Res.* **2009**, *48* (5), 239−256.
(46) Ginsberg, L.; Rafique, S.; Xuereb, J. H.; Rapoport, S. I.; Gershfeld, N. L. Disease and anatomic specificity of ethanolamine plasmalogen deficiency in Alzheimer's disease brain. *Brain Res.* **1995**, *698* (1−2), 223−226.
(47) Han, X.; Holtzman, D. M.; McKeel, D. W., Jr. Plasmalogen deficiency in early Alzheimer's disease subjects and in animal models: molecular characterization using electrospray ionization mass spectrometry. *J. Neurochem.* **2001**, *77* (4), 1168−1180.
(48) Plumb, R. S.; Johnson, K. A.; Rainville, P.; Smith, B. W.; Wilson, I. D.; Castro-Perez, J. M.; Nicholson, J. K. UPLC/MS(E); a new approach for generating molecular fragment information for biomarker structure elucidation. *Rapid Commun. Mass Spectrom.* **2006**, *20* (13), 1989−1994.
(49) Reddy, P. H.; Tripathi, R.; Troung, Q.; Tirumala, K.; Reddy, T. P.; Anekonda, V.; Shirendeb, U. P.; Calkins, M. J.; Reddy, A. P.; Mao, P.; Manczak, M. Abnormal mitochondrial dynamics and synaptic degeneration as early events in Alzheimer's disease: implications to mitochondria-targeted antioxidant therapeutics. *Biochim. Biophys. Acta, Mol. Basis Dis.* **2012**, *1822* (5), 639−649.
(50) Zhao, W.; Wang, J.; Varghese, M.; Ho, L.; Mazzola, P.; Haroutunian, V.; Katsel, P. L.; Gibson, G. E.; Levine, S.; Dubner, L.; Pasinetti, G. M. Impaired mitochondrial energy metabolism as a novel risk factor for selective onset and progression of dementia in oldest-old subjects. *Neuropsychiatr. Dis. Treat.* **2015**, *11*, 565−574.
(51) Swerdlow, R. H.; Burns, J. M.; Khan, S. M. The Alzheimer's disease mitochondrial cascade hypothesis. *J. Alzheimers Dis.* **2010**, *20* (S2), S265−S279.
(52) Navarro, E.; Romero, S. D.; Yaksh, T. L. Release of prostaglandin E2 from brain of cat: II. In vivo studies on the effects of adrenergic, cholinergic and dopaminergic agonists and antagonists. *Neuropharmacology* **1988**, *27* (10), 1067−1072.
(53) Gibson, G. E.; Xu, H.; Chen, H. L.; Chen, W.; Denton, T. T.; Zhang, S. Alpha-ketoglutarate dehydrogenase complex-dependent succinylation of proteins in neurons and neuronal cell lines. *J. Neurochem.* **2015**, *134* (1), 86−96.
(54) Gibson, G. E.; Blass, J. P.; Beal, M. F.; Bunik, V. The alpha-ketoglutarate-dehydrogenase complex: a mediator between mitochondria and oxidative stress in neurodegeneration. *Mol. Neurobiol.* **2005**, *31* (1−3), 43−63.
(55) Graham, S. F.; Holscher, C.; Green, B. D. Metabolic signatures of human Alzheimer's disease (AD): 1H NMR analysis of the polar metabolome of post-mortem brain tissue. *Metabolomics* **2014**, *10* (4), 744−753.
(56) Dautry, C.; Vaufrey, F.; Brouillet, E.; Bizat, N.; Henry, P. G.; Conde, F.; Bloch, G.; Hantraye, P. Early N-acetylaspartate depletion is a marker of neuronal dysfunction in rats and primates chronically treated with the mitochondrial toxin 3-nitropropionic acid. *J. Cereb. Blood Flow Metab.* **2000**, *20* (5), 789−799.
(57) Ebisu, T.; Rooney, W. D.; Graham, S. H.; Weiner, M. W.; Maudsley, A. A. N-acetylaspartate as an in vivo marker of neuronal viability in kainate-induced status epilepticus: 1H magnetic resonance spectroscopic imaging. *J. Cereb. Blood Flow Metab.* **1994**, *14* (3), 373−382.
(58) Glodzik, L.; Sollberger, M.; Gass, A.; Gokhale, A.; Rusinek, H.; Babb, J. S.; Hirsch, J. G.; Amann, M.; Monsch, A. U.; Gonen, O. Global N-acetylaspartate in normal subjects, mild cognitive impairment and Alzheimer's disease patients. *J. Alzheimers Dis.* **2015**, *43* (3), 939−947.
(59) Jaarsma, D.; Veenma-van der Duin, L.; Korf, J. N-acetylaspartate and N-acetylaspartylglutamate levels in Alzheimer's disease postmortem brain tissue. *J. Neurol. Sci.* **1994**, *127* (2), 230−233.
(60) Hampel, H.; Frank, R.; Broich, K.; Teipel, S. J.; Katz, R. G.; Hardy, J.; Herholz, K.; Bokde, A. L.; Jessen, F.; Hoessler, Y. C.; Sanhai, W. R.; Zetterberg, H.; Woodcock, J.; Blennow, K. Biomarkers for Alzheimer's disease: academic, industry and regulatory perspectives. *Nat. Rev. Drug Discovery* **2010**, *9* (7), 560−574.
(61) Jessen, F.; Traeber, F.; Freymann, K.; Maier, W.; Schild, H. H.; Block, W. Treatment monitoring and response prediction with proton MR spectroscopy in AD. *Neurology* **2006**, *67* (3), 528−530.
(62) Modrego, P. J.; Pina, M. A.; Fayed, N.; Diaz, M. Changes in metabolite ratios after treatment with rivastigmine in Alzheimer's

DOI: 10.1021/acs.jproteome.5b01020
J. Proteome Res. 2016, 15, 608−618

disease: a nonrandomised controlled trial with magnetic resonance spectroscopy. *CNS Drugs* **2006**, *20* (10), 867−877.
(63) Kalra, V.; Mittal, R. Duration of antiepileptic drug (AED) therapy. *Indian J. Pediatr.* **1998**, *65* (5), 772−775.

DOI: 10.1021/acs.jproteome.5b01020
J. Proteome Res. 2016, 15, 608−618